



HAL
open science

Hyperfine induced intensity redistribution in In

Jon Grumer, Martin Andersson, Tomas Brage

► **To cite this version:**

Jon Grumer, Martin Andersson, Tomas Brage. Hyperfine induced intensity redistribution in In. Journal of Physics B: Atomic, Molecular and Optical Physics, 2010, 43 (7), pp.74012. 10.1088/0953-4075/43/7/074012 . hal-00569892

HAL Id: hal-00569892

<https://hal.science/hal-00569892>

Submitted on 25 Feb 2011

HAL is a multi-disciplinary open access archive for the deposit and dissemination of scientific research documents, whether they are published or not. The documents may come from teaching and research institutions in France or abroad, or from public or private research centers.

L'archive ouverte pluridisciplinaire **HAL**, est destinée au dépôt et à la diffusion de documents scientifiques de niveau recherche, publiés ou non, émanant des établissements d'enseignement et de recherche français ou étrangers, des laboratoires publics ou privés.

Hyperfine induced intensity redistribution in In II

Jon Grumer^{1,2}, Martin Andersson^{2,3} and Tomas Brage¹

¹ Department of Physics, Lund University, Sweden

² Shanghai EBIT Laboratory, Institute of Modern Physics, Fudan University, Shanghai, People's Republic of China

³ The Key Laboratory of Applied Ion Beam Physics, Ministry of Education, People's Republic of China

E-mail: Tomas.Brage@fysik.lu.se

Abstract. We present a theoretical investigation of the hyperfine structure of the $5s5d\ ^3D_2 - 5s4f\ ^3F_{2,3}^o$ transitions in In II. Earlier work has failed in determining hyperfine constants for the upper levels of these transitions. We show that this is due to strong off-diagonal hyperfine interaction, which not only changes the position of the individual hyperfine lines, but also introduces large intensity redistributions among the different hyperfine levels. We present hyperfine dependent gf-values and show that off-diagonal hyperfine interaction reduces some of the gf-values by two orders of magnitude, while others are increased by up to more than a factor of 6. We also discuss the influence on the hyperfine structure of an accurate representation of the level-splitting of the $5s4f$ configuration. We show that the hyperfine interaction in $^3F_3^o$ and $^1F_3^o$ is very hard to determine accurately even in a large scale calculation and we derive a semi-empirical method for adjusting our results using an experimentally known, diagonal hyperfine constant for $5s4f\ ^1F_3^o$. The resulting theoretical synthetic spectra reproduces the experimental to high accuracy and facilitate identification of all observed lines.

PACS numbers: 31.15.A-, 32.10.Fn, 32.70.Cs, 32.70.Jz

1. Introduction

The hyperfine interaction can either result in an asymmetric broadening of the lines in a spectrum or even in new “unexpected” hyperfine induced lines if the hyperfine interaction is strong and the resolution is high. In high resolution stellar spectra, many lines are broadened due to the hyperfine interaction. As the resolution is improved, the demand on our detailed understanding of line shapes is increased, to be able to extract more accurate information. As an example, it is important to include hyperfine splitting in abundance analysis (Booth and Blackwell [1]). Jomaron *et al.* [2] showed that the abundance of Mn in chemically peculiar HgMn stars can be overestimated by 2 to 3 orders of magnitude if the hyperfine structure is not taken into consideration. It was also shown that if the hyperfine structure is included in a crude model, the abundance can still be wrong by a factor of 4. To improve the analysis of spectra of HgMn stars, the hyperfine structure of important elements have been experimentally studied in laboratories, for example Ga II by Karlsson and Litzén [3] and Mn I by Blackwell-Whitehead *et al.* [4]. Nb plays an important role in studies of the chemical evolution of heavy elements (Smith and Wallerstein [5] and Smith and Lambert [6]). To improve this analysis an experimental investigation of the hyperfine structure of Nb II was recently performed by Nilsson and Ivarsson [7].

The hyperfine interaction is often described in terms of A and B hyperfine constants. These can be determined experimentally through a fitting procedure to the spectrum (see for example Aboussaïd *et al.* [8]). This is a good approximation if the splitting of the fine structure levels are much larger than the hyperfine splitting. Aboussaïd *et al.* [8] analyzed the hyperfine structure of the $3d^24s - 3d4s4p$ transitions in Sc I and showed that when the fine structure and hyperfine structure are of the same order of magnitude, the off-diagonal hyperfine interaction can lead to strong intensity redistribution among the hyperfine lines in the spectrum.

Karlsson and Litzén [3] made an attempt to determine the A and B hyperfine constants for some transitions of astrophysical interest in Ga II. They found that this could not be done for the $4s4d - 4s4f$ transitions and they suggested that this was due to strong off-diagonal hyperfine interaction. Andersson *et al.* [9] performed calculations including the off-diagonal hyperfine interaction and could reproduce the experimental spectrum of the $4s4d - 4s4f$ transitions by Karlsson and Litzén [3]. Recently, Andersson [10] showed that similar cases can be expected for hyperfine transitions between terms with high angular momentum L , where the upper levels belongs to a configuration with an open s-shell. To be able to further investigate the hyperfine interaction in these types of systems we are developing a set of programs connected to the GRASP2K atomic structure program (Jönsson *et al.* [11]).

Karlsson and Litzén [12] investigated the hyperfine structure of In II, in an attempt to determine the A and B hyperfine constants. They found that the $5s5d \ ^3D_2 - 5s4f \ ^3F_{2,3}^o$ transitions could not be described by these diagonal constants and as a first test of our programs we have investigated the hyperfine structure of these transitions

and tried to reproduce the experimental spectrum by Karlsson and Litzén [12].

Paschen and Campbell [13] made an extensive analysis of the In II system, determining energies for a large number of levels belonging to configurations of the form $5snl$ with n up to 19 for low l value and up to $14h$ for high l . They found that almost all lines in the spectrum showed hyperfine structure and formed groups of lines that extended over several cm^{-1} . They also found that the observed interval between the hyperfine lines did not follow the predictions from theory and therefore they were not able to determine hyperfine constants in these cases. The deviation was interpreted as perturbations between different hyperfine levels. However, Paschen and Campbell [13] only took the nuclear magnetic dipole hyperfine interaction into consideration and left out the electric quadrupole, i.e. they tried to fit the hyperfine structure only using A hyperfine constants. The hyperfine structure of some low lying states has been determined using both the A and the B constants. Peik *et al.* [14] determined the hyperfine constants for $5s5p\ ^3P_1^o$, Larkins and Hannaford [15] determined the constants for $5s5p\ ^3P_{0,1,2}^o$ and $5s6s\ ^3S_1$ and Karlsson and Litzén [12] determined the constants for a wide range of levels. On the theoretical side, Jönsson and Andersson [16] calculated the hyperfine constants for a large number of low lying states in In II. Some work has also been performed concerning the off-diagonal hyperfine interaction. Zanthier *et al.* [17, 18] studied the hyperfine induced $5s^2\ ^1S_0 - 5s5p\ ^3P_0^o$ transition in connection with the work of constructing an ultra precise optical clock.

The off-diagonal hyperfine interaction can not only result in intensity redistribution among the hyperfine lines, but can also induce new types of transition channels. For example are the ground state and the first excited states in Beryllium, Magnesium and Zinc like ions of the type $ns^2\ ^1S_0$ and $nsnp\ ^3P_0^o$ respectively. These excited states can therefore not decay through any type of one-photon transition, but can only spontaneously decay through a two-photon decay, making the lifetime of these states very long. However, in the presence of a nuclear spin, the hyperfine interaction with the $nsnp\ ^3P_1^o$ and $nsnp\ ^1P_1^o$ states respectively will open a so called hyperfine induced electric dipole transition to the ground state, lowering the lifetime substantially. A theoretical investigation of the hyperfine quenching of $2s2p\ ^3P_0^o$ in Be-like ions was performed by Marques *et al.* [19]. Later, Brage *et al.* [20] performed a similar study showing that the model used by Marques *et al.* [19] was not valid. The lifetime of the $2s2p\ ^3P_0^o$ level in $^{47}\text{Ti}^{18+}$ was recently measured by Schippers *et al.* [21] and the Be-like iso-electronic sequence was re-investigated with improved models by both Cheng *et al.* [22] and Andersson *et al.* [23]. The Mg-like iso-electronic sequence has earlier been investigated by Marques *et al.* [24] and Brage *et al.* [20] and some disagreements were found. Recently the lifetime of the $3s3p\ ^3P_0^o$ level in $^{27}\text{Al}^+$ was measured by Rosenband *et al.* [25] and Andersson *et al.* [26] performed a new theoretical investigation of the Mg-like iso-electronic sequence finding agreement with the experimental result by Rosenband *et al.* [25] and explaining the earlier problems with the calculations by Marques *et al.* [24] and Brage *et al.* [20]. The Zn-like iso-electronic sequence has also been investigated by Liu *et al.* [27].

Much work has also been performed concerning hyperfine quenching of the third excited level, $1s2p\ ^3P_0^o$, in He-like ions. Johnson *et al.* [28] performed calculations for the whole iso-electronic sequence and Indelicato *et al.* [29] performed calculations for all ions with $Z > 40$. Many lifetime measurements of hyperfine quenched $1s2p\ ^3P_0^o$ levels in He-like ions has also been performed. For example in ^{19}F by Engström *et al.* [30], ^{27}Al Denne *et al.* [31], ^{31}P Livingston and Hinterlong [32] and ^{61}Ni Dunford *et al.* [33].

Not only hyperfine levels derived from a $J = 0$ fine structure level can have their lifetimes affected by hyperfine interaction. Bergström *et al.* showed that the lifetimes of the hyperfine levels belonging to the $6s19d\ ^3D_2$ and 1D_2 states in ^{87}Sr are heavily affected by the off-diagonal hyperfine interaction. Yao *et al.* [35, 36] predicted that the hyperfine levels of the $3d^94s\ ^3D_3$ levels in $^{129}\text{Xe}^{26+}$ should vary due to hyperfine quenching. This was later experimentally confirmed by Träbert *et al.* [37].

Besides introducing intensity redistribution and opening new transition channels, the off-diagonal hyperfine interaction can also change the energies of levels. For example is the diagonal hyperfine interaction for the $1s2p\ ^3P_0^o$ level in He-like ions zero. However, the off-diagonal hyperfine interaction with the $1s2p\ ^3P_1^o$ level is in some cases so strong that it substantially lower the energy of the $^3P_0^o$ state. This has been determined experimentally for $^{107}\text{Ag}^{45+}$ by Marrus *et al.* [38].

In this paper we report on off-diagonal hyperfine interaction in excited states in In II. This will result in pronounced line shifts, oscillator strength redistribution and the appearance of otherwise forbidden or unexpected lines in the $5s5d\ ^3D_2 - 5s4f\ ^3F_{2,3}^o$ transition arrays. In spite of the fact that the resulting structure is very complex, we will construct a model to explain, model and reproduce even details of the structure.

2. Theory

2.1. Hyperfine interaction

The interaction between the electrons and the electromagnetic multipole moments of the nucleus splits each fine structure level into multiple hyperfine levels. The interaction couples the nuclear spin, \mathbf{I} , and the total electronic angular momentum, \mathbf{J} , to a new total angular momentum, $\mathbf{F} = \mathbf{I} + \mathbf{J}$, and the hyperfine levels are denoted by their value of the corresponding quantum number, F .

The hyperfine interaction operator can be written as (Lindgren and Rosén [39])

$$\mathcal{H}_{hpf} = \sum_k \mathbf{T}^{(k)} \cdot \mathbf{M}^{(k)}, \quad (1)$$

where $\mathbf{T}^{(k)}$ and $\mathbf{M}^{(k)}$ are spherical tensor operators of rank k that operates on the electronic and the nuclear part of the wave function respectively. In this work we have included the first two terms in this expansion where $k = 1$ represents nuclear magnetic dipole and $k = 2$ the nuclear electric quadrupole interaction. The hyperfine interaction matrix element between two hyperfine levels $|\gamma I J F M_F\rangle$ and $|\gamma' I' J' F M_F\rangle$ thus consists

of two terms,

$$\langle \gamma I J F M_F | \mathcal{H}_{hpf} | \gamma' I' J' F M_F \rangle = W_{M1} + W_{E2}. \quad (2)$$

Hyperfine level dependent wave functions can be constructed by coupling the total electronic wave function, $|\gamma J M_J\rangle$, and the nuclear wave function $|I M_I\rangle$, using standard angular momentum coupling theory. It can then easily be shown that the two types of hyperfine interaction is represented by

$$W_{M1} = (-1)^{I+J+F} \left\{ \begin{array}{ccc} I & J & F \\ J' & I & 1 \end{array} \right\} \langle \gamma J \| T^{(1)} \| \gamma' J' \rangle \langle I \| M^{(1)} \| I \rangle \quad (3)$$

and

$$W_{E2} = (-1)^{I+J+F} \left\{ \begin{array}{ccc} I & J & F \\ J' & I & 2 \end{array} \right\} \langle \gamma J \| T^{(2)} \| \gamma' J' \rangle \langle I \| M^{(2)} \| I \rangle, \quad (4)$$

We can use the standard definitions of the nuclear magnetic dipole moment, $\mu_I = \langle I I | M_0^{(1)} | I I \rangle$, and the nuclear electric quadrupole moment, $Q = 2 \langle I I | M_0^{(2)} | I I \rangle$, to evaluate the reduced nuclear elements, i.e.

$$\langle I \| M^{(1)} \| I \rangle = \mu_I \sqrt{\frac{(2I+1)(I+1)}{I}} \quad (5)$$

$$\langle I \| M^{(2)} \| I \rangle = \frac{Q}{2} \sqrt{\frac{(2I+3)(I+1)(2I+1)}{I(2I-1)}}. \quad (6)$$

In this work we use values of μ_I and Q as tabulated by Kurucz [40].

2.2. The Hyperfine Constants

The hyperfine interaction is often viewed as a first-order perturbation to the energy, only requiring zero order wave function, i.e. pure JIF states. This is equivalent to only include the diagonal matrix elements of the hyperfine interaction matrix in the calculations. The hyperfine interaction energy contribution to a certain hyperfine level $|\gamma JIFM_F\rangle$ is then given by

$$\begin{aligned} \langle \gamma JIFM_F | \mathbf{T}^{(1)} \cdot \mathbf{M}^{(1)} + \mathbf{T}^{(2)} \cdot \mathbf{M}^{(2)} | \gamma JIFM_F \rangle = \\ = (1/2)AC + B \left[C(C+1) - (4/3)J(J+1)I(I+1) \right], \end{aligned} \quad (7)$$

where A and B are the hyperfine constants related to the magnetic dipole and electric quadrupole hyperfine interaction respectively, and $C = F(F+1) - J(J+1) - I(I+1)$.

However, this method is not sufficient when the off-diagonal hyperfine interaction is strong and the energy separations between the fine structure levels are small. This occurs typically for a configuration with an occupied orbital of high orbital angular momentum, leading to small fine structure, and open s-sub shells, inducing strong hyperfine interaction. As we will see, these configurations often also have term splitting of the same order of magnitude as the fine structure, and therefore will show pure coupling neither in the jj- or the LS-case, complicating the picture even further.

2.3. Transition Probability

The weighted oscillator strength, or the gf -value, between two hyperfine levels $|\Gamma JIF\rangle$ and $|\Gamma' J'IF'\rangle$, can be written as

$$gf = \frac{8\pi^2 m_e c a_0^2 \sigma}{3h} \left| \langle \Gamma JIF \| \mathbf{D}^{(1)} \| \Gamma' J'IF' \rangle \right|^2, \quad (8)$$

using standard notations. The wave functions describing a hyperfine level, $|\Gamma JIF\rangle$, is constructed as a linear combination of pure JIF coupled basis functions, $|\gamma JIF\rangle$. Rewriting $|\Gamma JIF\rangle$ and $|\Gamma' J'IF'\rangle$ in form of their expansion, the gf -value is given by

$$gf = \frac{8\pi^2 m_e c a_0^2 \sigma}{3h} \left| \sum_{\gamma J} \sum_{\gamma' J'} c_{\gamma J} c_{\gamma' J'} \langle \gamma JIF \| \mathbf{D}^{(1)} \| \gamma' J'IF' \rangle \right|^2, \quad (9)$$

where c :s represents the expansion coefficients in the basis functions for the upper and lower state, respectively. The matrix elements in this equation can be expressed in terms of reduced matrix elements, which only depends on the electronic part of the wave function, as

$$\begin{aligned} \langle \gamma JIF \| \mathbf{D}^{(1)} \| \gamma' J'IF' \rangle &= (-1)^{J+J'+F'+1} \sqrt{(2F+1)(2F'+1)} \\ &\times \begin{Bmatrix} F & J & I \\ J' & F' & 1 \end{Bmatrix} \langle \gamma J \| \mathbf{D}^{(1)} \| \gamma' J' \rangle. \end{aligned} \quad (10)$$

Combining (9) and (10) yields

$$\begin{aligned} gf &= \frac{8\pi^2 m_e c a_0^2 \sigma}{3h} (2F+1)(2F'+1) \left| \sum_{\gamma J} \sum_{\gamma' J'} (-1)^J c_{\gamma J} c_{\gamma' J'} \right. \\ &\quad \times \begin{Bmatrix} F & J & I \\ J' & F' & 1 \end{Bmatrix} \langle \gamma J \| \mathbf{D}^{(1)} \| \gamma' J' \rangle \left. \right|^2. \end{aligned} \quad (11)$$

3. The MCDHF method

Throughout this work, we used the Multi-Configuration Dirac-Hartree-Fock method (MCDHF) [42], in the form of the GRASP2K relativistic atomic structure package, Jönsson *et al.* [11]. The MCDHF method is based on the fundamental assumption that the Atomic State Function (ASF) $|\Gamma JM_J\rangle$ can be expressed as a linear combination of Configuration State Functions (CSF:s) as

$$|\Gamma JM_J\rangle = \sum_i c_i |\gamma_i JM_J\rangle. \quad (12)$$

The CSF:s are in turn wave functions constructed as a coupled and anti-symmetric sum of products of one electron wave functions, so called Dirac orbitals which can be expressed as

$$\phi(r, \theta, \varphi, \sigma) = \frac{1}{r} \begin{pmatrix} P(r) \chi_{\kappa m}(\theta, \varphi, \sigma) \\ iQ(r) \chi_{-\kappa m}(\theta, \varphi, \sigma) \end{pmatrix}. \quad (13)$$

The spin and angular dependent parts of the Dirac orbitals, $\chi_{\kappa m}(\theta, \varphi, \sigma)$ and $\chi_{-\kappa m}(\theta, \varphi, \sigma)$ are assumed to be known and the radial parts $P(r)$ and $Q(r)$ remain to be determined.

Starting from the Dirac-Coulomb Hamiltonian the ASF:s were optimized to self consistency in an iterative procedure where both the radial parts of the Dirac orbitals and the expansion coefficients c_i were optimized. In a subsequent Configuration Interaction (CI) calculation (McKenzie *et al.* [43]), the zero-frequency limit of the Breit interaction and the leading QED effects were included.

To simplify our notations when we later include hyperfine interaction in our model, we define the optimized ASF:s from the Dirac-Coulomb Hamiltonian as J-state functions (JSF:s). These should describe the fine structure levels in an isotope without a nuclear spin. From the JSF:s a number of atomic properties such as the reduced hyperfine interaction matrix elements and the transition matrix elements could be evaluated as expectation values. The transitions of interest were calculated between JSF:s described by independently optimized Dirac-orbitals. To be able to evaluate these, bi-orthogonal transformation (Olsen *et al.* [44]) had to be performed. In the new representation, the transition matrix elements in the Babushkin or Coulomb gauge could be calculated using standard Racah algebra techniques (Grant [45]).

4. Method of calculation

4.1. Optimization of wave functions

The calculations were performed using the Restricted Active Space method, Roos *et al.* [46], Olsen *et al.* [47] and Brage and Fischer [48]. This method is an orbital driven technique where the calculations are expanded in a systematic manner. In each step the configuration space is expanded by including configurations formed by allowing for excitations from one or more reference configurations to a certain set of Dirac orbitals. This method has been proven to be well suited for studying the convergence of the calculations, as well as for investigating the importance of including various types of correlations.

The even ($5s5d$) and the odd ($5s4f$) levels were optimized in two separate calculations. Beginning with the even, we started from a Dirac-Hartree-Fock calculation where all relativistic forms of the $5s5d$ configuration were included and the Dirac orbitals were optimized. The calculation was then extended by expanding our configuration space by including all configurations which could be formed by allowing for single and double excitations from the multi-reference set $5s5d$ and $5p^2$ to certain sets of Dirac orbitals. The systematic approach made it possible to investigate the importance of different types of correlations. In our final model valence and core-valence correlation with $4d$ was included. The configuration space then included all configurations of the form

$$4d^{10}nln'l', \quad 4d^95snln'l', \quad 4d^95pnln'l', \quad 4d^95dnl'n'l',$$

where nl and $n'l'$ in each step belonged to the sets of orbitals

$$\begin{aligned} AS1 &= \{4f, 5s, 5p, 5d\}, \\ AS2 &= AS1 + \{5f, 5g, 6s, 6p, 6d\}, \\ AS3 &= AS2 + \{6f, 6g, 7s, 7p, 7d\}, \\ AS4 &= AS3 + \{7f, 7g, 8s, 8p, 8d\}. \end{aligned}$$

In each step only the new orbitals were optimized whereas the old were kept fixed.

The calculation for the odd level was performed in a similar way. The configuration space was created by allowing for single and double excitations from the reference configuration $5s4f$, i.e. included all configurations of the form

$$4d^{10}nl'n'l', \quad 4d^94fnln'l', \quad 4d^95snln'l'.$$

After the wave functions had been optimized, the zero-frequency limit of the Breit interaction and the leading QED effects were included in a CI-calculation, that is without orbital optimization. We used the JSF:s from these calculations to evaluate reduced transition matrix elements between the $5s4f$ and $5s5d$ levels. Finally, by using a subprogram of HFSZEEMAN (Andersson and Jönsson [49]) we computed reduced nuclear magnetic and electric quadrupole hyperfine interaction matrix elements.

It has been shown (Lindgren and Morrison [50] and Jönsson [51]) that hyperfine interaction is often sensitive to so called spin-polarization. This is represented in an efficient way by allowing for single excitations from inner s-subshells and a small mixing with such a state can have a substantial impact on the size of the hyperfine interaction. To account for this effect one further step was added to the optimization of the even and odd levels. In this step we included one additional s-orbital and added all configurations which could be formed by allowing for one excitation from the $1s$, $2s$, $3s$ or $4s$ shell and at the most one excitation from a valence electron. In this step only the new s-orbital was varied. Again, we finished also this step with a Breit-QED CI calculation and used the resulting JSF:s to evaluate reduced hyperfine interaction elements.

4.2. Hyperfine Structure

The hyperfine interaction was calculated using our newly developed program HFSMIX, which is a modified version of a subprogram of HFSZEEMAN, Andersson and Jönsson [49]. Starting from the J-state function we construct *hyperfine configuration state functions* (HCSF) using standard coupling theory. Using these together with the matrices of the reduced magnetic dipole and electric quadrupole hyperfine interaction matrix elements, HFSMIX calculates the energies and the corresponding final atomic state functions, the *F-state functions* (FSF).

The hyperfine structure calculations discussed so far were completely ab initio. Recreating the energy splittings within the configurations was however a true challenge, since In II represents a relatively heavy ion of low ionization stage. Our goal was to reproduce an experimental spectrum, i.e. the hyperfine transition energies and the

corresponding gf-values which are affected by strong off-diagonal hyperfine interaction. To do this an accurate representation of the J-dependent energy spectrum was necessary. We therefore re-scaled the GRASP2K fine structure energies to experimental center-of-intensity values found by Karlsson and Litzén [12]. The asymmetric broadening effect of the hyperfine interaction, which was not considered by Karlsson and Litzén, allowed us to modify these values even further.

Since hyperfine levels with different F quantum number can not mix, it was convenient to performed the calculations in block form. An interaction matrix was created for each F -value using (3) and (4) and then diagonalized, which yielded new hyperfine level energies as well as the corresponding expansion coefficients of the hyperfine configuration state functions, describing the F-state function. Using these wave functions, the gf-values were calculated using a newly written program, HFSTRANS, that is based on equation (11) where the electric dipole transition reduced matrix elements were calculated using GRASP2K.

4.3. Spectrum Generation

The line intensities of a spectrum from a hollow cathode light source, as used by Karlsson and Litzén [3], should be proportional to the gf-values (assuming that the radiative rates are much larger than the competing collision rates). A synthetic spectrum may then be generated by giving the lines gaussian profiles, due to doppler broadening, with a given Full Width Half Maximum, FWHM.

We only considered one of the stable isotopes, ^{115}In , in this work, since ^{113}In has a low abundance (4.3%) and the two isotopes have very similar nuclear properties. They have the same nuclear spin $9/2$, ^{115}In has a nuclear magnetic dipole moment of $\mu_I = 5.5408$ and a nuclear electric quadrupole moment of $Q = 0.861$, whereas ^{113}In has the nuclear moments $\mu_I = 5.5289$ and $Q = 0.846$ (Kurucz [40]). Furthermore, since the FWHM of the lines is proportional to $1/\sqrt{M}$ the width will only differ by 0.9%. The errors due to neglecting one of the isotopes was therefore well within our uncertainty estimates.

5. Results and discussion

In Table 1 and 2 we present convergence studies of some atomic properties of interest for the optimizations of the JSF:s. In Table 1 we study the convergence of the energy splitting within $5s4f$ as the configuration space is expanded. In this table *ASX* refers to the different steps in the calculations. From this table it is found that we achieved a fairly good convergence for the energy splittings between *AS3* and *AS4*. Comparing with experimental energies by Karlsson and Litzén [12] it is found that our calculated energy splitting between $5s4f\ ^3F_3^o$ and $^1F_3^o$ is close to the experimental value whereas large discrepancies are found for the fine structure splitting. These splittings are however not crucial, since we adjust the energies to experimental values, before including hyperfine

Table 1. A convergence study of the energy splitting among the $5s4f$ levels relative to ${}^3F_2^o$. All energies given in cm^{-1} .

	$\Delta E_{3F_3^o}$	$\Delta E_{3F_4^o}$	$\Delta E_{1F_3^o}$
AS1	14.34	58.66	175.98
AS2	3.93	13.10	96.30
AS3	2.53	9.92	53.47
AS4	2.66	10.50	52.26
Exp ^a	4.92	21.65	56.02

^a Karlsson and Litzén [12]

Table 2. A convergence study of the gf-values of the $5s5d\ {}^3D_2 - 5s4f\ {}^3F_{2,3}^o$ transitions.

	${}^3D_2 - {}^3F_2^o$		${}^3D_2 - {}^3F_3^o$	
	Coul.	Bab.	Coul.	Bab.
AS1	0.3605	0.7328	2.835	5.542
AS2	0.4704	0.6120	3.708	4.823
AS3	0.4905	0.5777	3.796	4.475
AS4	0.4923	0.5643	3.799	4.356

interaction.

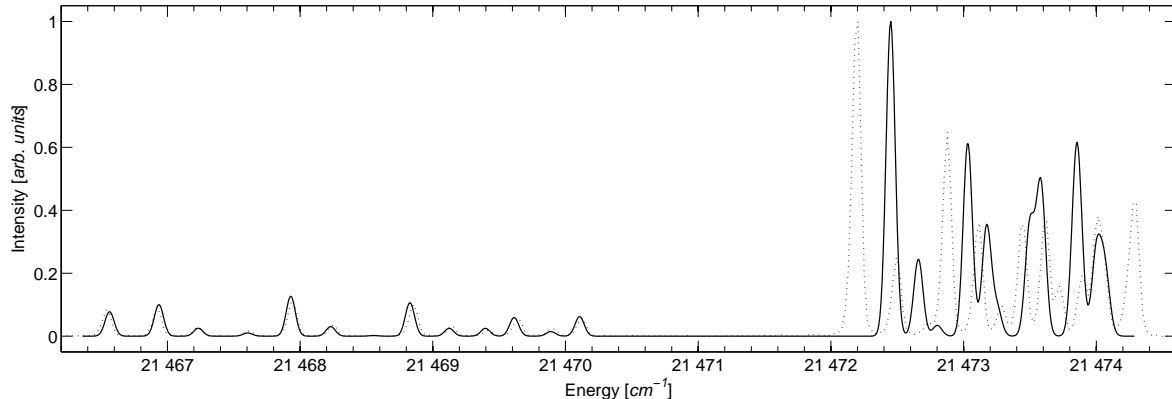
In Table 2 we investigate the convergence of the gf-values for the two transitions we focus on in this work, using both the Coulomb and the Babushkin form of the transition operator. For exact wave functions, these should be identical. Therefore a comparison of the two is an indicator of the accuracy of our calculations. Here the Babushkin gauge corresponds to the length form in the non-relativistic limit and is in general considered to give the most reliable results. From Table 2 it is found that good convergence is obtained between AS3 and AS4. Comparing the Coulomb and the Babushkin results it is found that the former are 13% smaller than the latter for both transitions.

5.1. Spectra of hyperfine lines

In Figure 1 we present our synthetic spectrum (solid line) compared to the experimental one by Karlsson and Litzén [12] (dotted line). In this figure the left group of lines represents hyperfine components of the $5s5d\ {}^3D_2 - 5s4f\ {}^3F_2^o$ transition, whereas the right represents the components of the $5s5d\ {}^3D_2 - 5s4f\ {}^3F_3^o$ transition. It is clear that while the former agrees well with the experimental spectrum, the latter shows strong discrepancies.

The discrepancies of the hyperfine structure of the $5s5d\ {}^3D_2 - 5s4f\ {}^3F_3^o$ transition can be understood from an investigation of the calculated A hyperfine interaction constants. In Table 3 we present a convergence study of how the different hyperfine constants of $5s4f$ varied as the calculation was expanded. Studying $A({}^3F_2^o)$ and $A({}^3F_4^o)$

Figure 1. Our synthetic spectrum (solid line) compared to experimental spectrum by Karlsson and Litzén [12] (dotted line). Left group of peaks is the hyperfine components of the $5s5d\ ^3D_2 - 5s4f\ ^3F_2^o$ transitions and the right group is the $^3D_2 - ^3F_3^o$.



it is found that the values change significantly between the two first steps and then seems to converge. Between $AS4$ and $AS4_{sp}$ there are also some changes. This is due to the inclusion of the spin-polarization which in general increases the size of the hyperfine interaction. These values are not part of the convergence study but should be compared to experimental values if available. Studying $A(^3F_3^o)$ and $A(^1F_3^o)$ we find large deviations between the different steps, but between $AS3$ and $AS4$ a fair convergence is obtained. However, comparing $A(^1F_3^o)$ to the experimental value by Karlsson and Litzén [12], it is found that our value is significantly too low.

In Table 3 we also present how the sum of $A(^3F_3^o)$ and $A(^1F_3^o)$ varies as the calculation is expanded and it is found that this sum is just as stable as the hyperfine constants $A(^3F_2^o)$ and $A(^3F_4^o)$. The reason for this is that that $A(^3F_3^o)$ and $A(^1F_3^o)$ are very sensitive to the mixing coefficients of the $(5s4f_{5/2})_3^o$ and $(5s4f_{7/2})_3^o$ CSF:s in the JSF:s describing $5s4f\ ^3F_3^o$ and $^1F_3^o$, since the hyperfine constants for the pure CSF:s are 3030.9 and -2272.5MHz respectively. The sum of these constants is 758.4MHz , i.e. about the same as the sum of $A(^3F_3^o)$ and $A(^1F_3^o)$ through the different steps of the calculation. We will show that this can be used to adjust our hyperfine interaction matrix elements.

The hyperfine structure of the lower $5s5d\ ^3D_2$ level can also be described by hyperfine constants and our theoretical value of $A(^3D_2) = 1796\text{MHz}$ is close to the experimental value of 1865MHz by Karlsson and Litzén [12]. The slightly too small value for this hyperfine interaction matrix element is the main reason why the structure of the $5s5d\ ^3D_2 - 5s4f\ ^3F_2^o$ transition is too narrow in our calculation compared to the experiment.

Table 3. A convergence study of the A hyperfine constants for the $5s4f$ levels. All constants are given in MHz .

	$A(^3F_2^o)$	$A(^3F_3^o)$	$A(^1F_3^o)$	$A(^3F_4^o)$	$A(^3F_3^o) + A(^1F_3^o)$
AS1	-2888	-578.7	1320.2	2180	741.5
AS2	-3260	51.5	762.9	2452	830.4
AS3	-3215	-223.3	1036.6	2418	813.4
AS4	-3260	-278.4	1102.5	2452	824.1
$AS4_{sp}$	-3473	-327.6	1205.1	2612	877.5
Exp ^a					1736±21

^a Karlsson and Litzén [12]

5.2. Semi-Empirical Adjustments to the Calculation

In this section we will discuss a method that, through a semi-empirical re-scaling of some of the reduced nuclear magnetic dipole hyperfine interaction matrix elements, will address the problem of obtaining correct expansion coefficients of the $(5s4f_{5/2})_3^o$ and $(5s4f_{7/2})_3^o$ CSF:s describing the JSF:s of the states $5s4f$ $^1F_3^o$ and $^3F_3^o$. We start with a re-scaling of all the diagonal elements of the $5s4f$ $^3F_3^o$ and $^1F_3^o$ states. This changes the wave functions of the states of interest which makes it possible to also shift the off-diagonal elements. In a third and final step we re-scale the matrix elements of the $5s5d$ 3D_2 state as well, even though this has much less impact on the spectrum.

The adjustments done are based on the fact that the sum of the hyperfine constants $A(^1F_3^o)$ and $A(^3F_3^o)$ remains more or less constant throughout the the calculations, as discussed in the previous section. The idea behind the first adjustment is to re-scale two of the four hyperfine constants to semi-empirical values. Using the experimental value of $A(^1F_3^o)$ by Karlsson and Litzén [12], together with the fact that the sum of the $J=3$ A -constants are well determined, we can also indirectly re-scale $A(^3F_3^o)$. This will in turn give a scaling factor for the corresponding reduced matrix element. The other two diagonal elements, $\langle ^3F_4^o || \mathbf{T}^{(1)} || ^3F_4^o \rangle$ and $\langle ^3F_2^o || \mathbf{T}^{(1)} || ^3F_2^o \rangle$, are left unchanged, since the $^3F_4^o$ is not included in this study and $^3F_2^o$ is heavily dominated by one CSF and we can therefore assume that our value for the $A(^3F_2^o)$ is accurate.

The pure ab initio reduced matrix elements have the following values

$$\begin{pmatrix} 0.72546 & -0.67846 & 0.52425 & 0.00000 \\ 0.76930 & -0.07049 & 0.63344 & -0.51175 \\ -0.59445 & 0.63344 & 0.25931 & -0.66204 \\ 0.00000 & 0.60551 & 0.78334 & -0.52841 \end{pmatrix} \quad (14)$$

where the rows and columns are sorted as the J-states: $^3F_4^o$, $^3F_3^o$, $^1F_3^o$, $^3F_2^o$.

The electronic hyperfine interaction operator acts on one electron at a time, thus $\mathbf{T}^{(1)} = \sum_{i=1}^n \mathbf{t}^{(1)}(i)$ where n is the number of electrons. The contribution from the hyperfine interaction can therefore be written as

$$\begin{aligned}
& \langle I[(\alpha\tilde{J}_{n-1})j_n]JFM_F|\mathbf{T}^{(1)} \cdot \mathbf{M}^{(1)}|I[(\beta\tilde{J}'_{n-1})j'_n]J'FM_F\rangle = \\
& = (-1)^{I+J+F} \left\{ \begin{array}{ccc} I & J & F \\ J' & I & 1 \end{array} \right\} \\
& \quad \times \sum_i \langle [(\alpha\tilde{J}_{n-1})j_n]J\|\mathbf{t}^{(1)}(i)\|[(\beta\tilde{J}'_{n-1})j'_n]J'\rangle \langle I\|\mathbf{M}^{(1)}\|I\rangle
\end{aligned} \tag{15}$$

We are interested in calculating the interaction matrix elements between the CSF:s $(5s4f_{5/2})_{2,3}^o$ and $(5s4f_{7/2})_{3,4}^o$. In deriving the expression for performing these calculation we start by noting that there is no net contribution from electrons in closed shells and we will therefore only have a summation over two terms. By decoupling all spectator electrons we end up with the expression

$$\begin{aligned}
& \langle I[(\alpha 0, 5s_{1/2})1/2, 4f_j]JFM_F|\mathbf{T}^{(1)} \cdot \mathbf{M}^{(1)}|I[(\beta 0, 5s_{1/2})1/2, 4f_{j'}]J'FM_F\rangle = \\
& = (-1)^{I+J+F+3/2} \delta_{\alpha,\beta} \sqrt{(2J+1)(2J'+1)} \left\{ \begin{array}{ccc} I & J & F \\ J' & I & 1 \end{array} \right\} \langle I\|\mathbf{M}^{(1)}\|I\rangle \\
& \quad \times \left[(-1)^{j+J'} \delta_{4f_j, 4f_{j'}} \left\{ \begin{array}{ccc} 1/2 & j & J \\ J' & 1 & 1/2 \end{array} \right\} \langle 5s_{1/2}\|\mathbf{t}^{(1)}\|5s_{1/2}\rangle \right. \\
& \quad \left. + (-1)^{j'+J} \left\{ \begin{array}{ccc} 1/2 & j & J \\ 1 & J' & j' \end{array} \right\} \langle 4f_j\|\mathbf{t}^{(1)}\|4f_{j'}\rangle \right]
\end{aligned} \tag{16}$$

where α and β represents occupation numbers of sub-shells and all coupling information needed to uniquely define the configuration state functions.

Using equation (16) we can estimate the relative size of the interaction matrix elements between the four CSF:s $(5s4f_{5/2})_{2,3}^o$ and $(5s4f_{7/2})_{3,4}^o$. By performing Dirac-Fock calculations only including one CSF, the diagonal hyperfine interaction constants could be evaluated and it was found that $A((5s4f_{5/2})_3^o) = 3031 MHz$ and $A((5s4f_{7/2})_3^o) = -2272 MHz$ or $A((5s4f_{5/2})_3^o) = -1.334 \cdot A((5s4f_{7/2})_3^o)$. Using equation (16) and only including the contribution from the $5s$ electron, the relative size of the two hyperfine constants are determined by the 6j-symbol and would be $A((5s4f_{5/2})_3^o) = -4/3 \cdot A((5s4f_{7/2})_3^o)$. Including the contribution from the $4f$ shells would increase both of the hyperfine constants making the relative size smaller than $-4/3$. From this it is obvious that the contributions from the $4f$ shells are very small compared to the contribution from the $5s$ shell. This can also be understood from calculating the reduced one-electron matrix elements in equation (16) using hydrogenic orbitals. Assuming that the screening is the same in the three orbitals $5s$, $4f_{5/2}$ and $4f_{7/2}$, the relative size of the different reduced matrix elements would then be

$$\begin{aligned}
\langle 4f_{5/2}\|\mathbf{t}^{(1)}\|4f_{5/2}\rangle &= 8.17 \cdot 10^{-2} \langle 5s\|\mathbf{t}^{(1)}\|5s\rangle \\
\langle 4f_{7/2}\|\mathbf{t}^{(1)}\|4f_{7/2}\rangle &= 6.09 \cdot 10^{-2} \langle 5s\|\mathbf{t}^{(1)}\|5s\rangle \\
\langle 4f_{7/2}\|\mathbf{t}^{(1)}\|4f_{5/2}\rangle &= 6.59 \cdot 10^{-3} \langle 5s\|\mathbf{t}^{(1)}\|5s\rangle
\end{aligned}$$

However, to get a more reasonable screening for the $5s4f$ configuration In II we performed a Hartree-Fock calculation using the ATSP2K (Fischer *et al.* [52]). It was then found that the $5s$ electron see an average charge of about 15, whereas the $4f$ electron see a charge of about 2. Using a charge of 2 for both the $4f_{5/2}$ and the $4f_{7/2}$ orbitals the relative size between the different reduced one electron matrix elements are

$$\begin{aligned}\langle 4f_{5/2} || \mathbf{t}^{(1)} || 4f_{5/2} \rangle &= 1.94 \cdot 10^{-4} \langle 5s || \mathbf{t}^{(1)} || 5s \rangle \\ \langle 4f_{7/2} || \mathbf{t}^{(1)} || 4f_{7/2} \rangle &= 1.44 \cdot 10^{-4} \langle 5s || \mathbf{t}^{(1)} || 5s \rangle \\ \langle 4f_{7/2} || \mathbf{t}^{(1)} || 4f_{5/2} \rangle &= 1.56 \cdot 10^{-5} \langle 5s || \mathbf{t}^{(1)} || 5s \rangle\end{aligned}$$

From this it is clear that the $4f$ orbitals only plays a minor role for the hyperfine interaction in the system we are investigating. Following this discussion, the nuclear magnetic dipole hyperfine interaction matrix between the HCSF:s of the states $5s4f_{7/2}$ and $5s4f_{5/2}$ can schematically be represented by

$$\begin{pmatrix} \mathcal{E} & \mathcal{E} & \varepsilon & 0 \\ \mathcal{E} & \mathcal{E} & \varepsilon & \varepsilon \\ \varepsilon & \varepsilon & \mathcal{E} & \mathcal{E} \\ 0 & \varepsilon & \mathcal{E} & \mathcal{E} \end{pmatrix} \quad (17)$$

where the columns and rows are ordered according to configuration state functions $(5s4f_{7/2})_4^o$, $(5s4f_{7/2})_3^o$, $(5s4f_{5/2})_3^o$ and $(5s4f_{5/2})_2^o$. In this representation, ε symbolizes elements dominated by contributions from the $4f$ -interactions, i.e. depending on the reduced matrix element $\langle 4f_{7/2} || \mathbf{t}^{(1)} || 4f_{5/2} \rangle$, while the \mathcal{E} is dominated by contributions from $5s$ -interaction, depending on the element $\langle 5s_{1/2} || \mathbf{t}^{(1)} || 5s_{1/2} \rangle$. It is clear from the discussion above that the former is expected to be significantly smaller than the latter. One should be aware of that there also is a dependence on the 6-j symbols in (16). The main fluctuation however, comes from the electronic reduced matrix element.

We start by assuming that the J-state functions of ${}^3F_3^o$ and ${}^1F_3^o$ can be represented by a linear combinations of only the two CSF:S $(5s4f_{7/2})_3^o$ and $(5s4f_{5/2})_3^o$, i.e.

$$|5s4f {}^3F_3^o\rangle = a|(5s4f_{7/2})_3^o\rangle + b|(5s4f_{5/2})_3^o\rangle \quad (18)$$

$$|5s4f {}^1F_3^o\rangle = -b|(5s4f_{7/2})_3^o\rangle + a|(5s4f_{5/2})_3^o\rangle \quad (19)$$

The corresponding self interaction (diagonal) reduced matrix elements are then

$$\begin{aligned}\langle 5s4f {}^3F_3^o || \mathbf{T}^{(1)} || 5s4f {}^3F_3^o \rangle &= \\ &= a^2 \langle (5s4f_{7/2})_3^o || \mathbf{T}^{(1)} || (5s4f_{7/2})_3^o \rangle + b^2 \langle (5s4f_{5/2})_3^o || \mathbf{T}^{(1)} || (5s4f_{5/2})_3^o \rangle \\ &\quad + 2ab \langle (5s4f_{7/2})_3^o || \mathbf{T}^{(1)} || (5s4f_{5/2})_3^o \rangle \\ &\approx a^2 \langle (5s4f_{7/2})_3^o || \mathbf{T}^{(1)} || (5s4f_{7/2})_3^o \rangle + b^2 \langle (5s4f_{5/2})_3^o || \mathbf{T}^{(1)} || (5s4f_{5/2})_3^o \rangle\end{aligned} \quad (20)$$

$$\begin{aligned}\langle 5s4f {}^3F_3^o || \mathbf{T}^{(1)} || 5s4f {}^1F_3^o \rangle &= \dots \\ &\approx b^2 \langle (5s4f_{7/2})_3^o || \mathbf{T}^{(1)} || (5s4f_{7/2})_3^o \rangle + a^2 \langle (5s4f_{5/2})_3^o || \mathbf{T}^{(1)} || (5s4f_{5/2})_3^o \rangle\end{aligned} \quad (21)$$

where we have used that the $\langle (5s4f_{7/2})_3^o || \mathbf{T}^{(1)} || (5s4f_{5/2})_3^o \rangle$ element is of order ε and according to the discussion above these are small enough to be taken away.

Table 4. The *Ab Initio* and re-scaled hyperfine interaction constants and reduced matrix elements. The hyperfine constants are given in *MHz* and the reduced matrix elements in *au*. $\sum A = A(^1F_3^o) + A(^3F_3^o)$.

	$\langle ^1F_3^o \mathbf{T}^{(1)} ^1F_3^o \rangle$	$\langle ^3F_3^o \mathbf{T}^{(1)} ^3F_3^o \rangle$	$A(^1F_3^o)$	$A(^3F_3^o)$	$\sum A$
<i>AS4_{sp}</i>	0.25931	-0.07049	1205.07	-327.59	877.48
<i>Rescaled</i>	0.37356	-0.18473	1736 ^a	-858.52	877.48

^aKarlsson and Litzén [12]

We will start by only considering the contribution to the JSF:s from these two main CSF:s, in order to derive an adjustment procedure. This leads to that

$$a^2 + b^2 = 1 \quad (22)$$

and the sum of equation (20) and 21) reduces to

$$\begin{aligned} & \langle 5s4f \ ^3F_3^o || \mathbf{T}^{(1)} || 5s4f \ ^3F_3^o \rangle + \langle 5s4f \ ^3F_3^o || \mathbf{T}^{(1)} || 5s4f \ ^3F_3^o \rangle = \\ & = \langle (5s4f_{7/2})_3^o || \mathbf{T}^{(1)} || (5s4f_{7/2})_3^o \rangle + \langle (5s4f_{5/2})_3^o || \mathbf{T}^{(1)} || (5s4f_{5/2})_3^o \rangle. \end{aligned} \quad (23)$$

This implies that if we in the expansion of $|5s4f \ ^3F_3^o\rangle$ and $|5s4f \ ^1F_3^o\rangle$ only include $(5s4f_{7/2})_3^o$ and $(5s4f_{5/2})_3^o$, the sum of the two hyperfine interaction reduced matrix elements is constant and independent of expansion coefficients a and b . This fact of course immediately follows from that the trace of a square matrix is invariant under unitary transformations.

It is now straight forward to make a first semi-empirical approximation by re-scaling the hyperfine constants (see Table 4). When we have determined the scaling factors, we re-scale the two diagonal reduced matrix elements. The interaction matrix (14) is then changed into

$$\begin{pmatrix} 0.72546 & -0.67846 & 0.52425 & 0.00000 \\ 0.76930 & -0.18473 & 0.63344 & -0.51175 \\ -0.59445 & 0.63344 & 0.37356 & -0.66204 \\ 0.00000 & 0.60551 & 0.78334 & -0.52841 \end{pmatrix} \quad (24)$$

The re-scaling of the diagonal reduced nuclear magnetic dipole hyperfine interaction matrix elements can be used to adjust the mixing coefficients of the CSFs in the JSFs. These can be used to compute adjusted values for both the *off-diagonal* hyperfine interaction matrix elements as well as *transition* matrix elements.

To calculate the new mixing coefficients a' and b' we can not describe the JSF:s only in terms of the CSF:s $(5s4f_{7/2})_3^o$ and $(5s_{1/2}4f_{5/2})_3^o$, but have to add a "rest term" according to

$$|5s4f \ ^3F_3^o\rangle = a|(5s4f_{7/2})_3^o\rangle + b|(5s4f_{5/2})_3^o\rangle + \dots \quad (25)$$

$$|5s4f \ ^1F_3^o\rangle = -b|(5s4f_{7/2})_3^o\rangle + a|(5s4f_{5/2})_3^o\rangle + \dots \quad (26)$$

Table 5. Theoretical values of the A hyperfine constants of the pure CSF:s $|(5s4f_{7/2})_3^o\rangle$ and $|(5s4f_{5/2})_3^o\rangle$. Also given are the mixing coefficients of the two CSF:s in the JSF of $5s4f\ ^1F_3^o$ from the *AS4* calculation.

	A	mixing coeff.
$(5s4f_{7/2})_3^o$	-2272.46	$a = 0.7802$
$(5s4f_{5/2})_3^o$	3030.90	$b = 0.6026$
$\sum A$	758.44	
$a^2 + b^2$		0.9718

We can then express the corresponding hyperfine constants as

$$A(^3F_3^o) = a^2 A((5s4f_{7/2})_3^o) + b^2 A((5s4f_{5/2})_3^o) + \mathcal{O}(^3F_3^o) \quad (27)$$

$$A(^1F_3^o) = b^2 A((5s4f_{7/2})_3^o) + a^2 A((5s4f_{5/2})_3^o) + \mathcal{O}(^1F_3^o). \quad (28)$$

The corrected mixing coefficients a' and b' can now be derived by solving the equation,

$$A_{exp}(^1F_3^o) = b'^2 A((5s4f_{7/2})_3^o) + a'^2 A((5s4f_{5/2})_3^o) + \mathcal{O}(^1F_3^o) \quad (29)$$

under the condition

$$a^2 + b^2 = a'^2 + b'^2. \quad (30)$$

The rest term is here the same as in equation (28), since the corresponding part of the wave function is unaffected by our adjustments. From equation (29) we find that $\mathcal{O}(^1F_3^o) = 185.29\text{MHz}$. All other information to solve equation 29 is found in Table (4) and (5) and by choosing the solutions closest to the original values, we find that

$$a' = 0.8419 \quad (31)$$

$$b' = 0.5128 \quad (32)$$

With new values of the expansion coefficients, we find the following scaling factors for the off-diagonal elements of matrix (24)

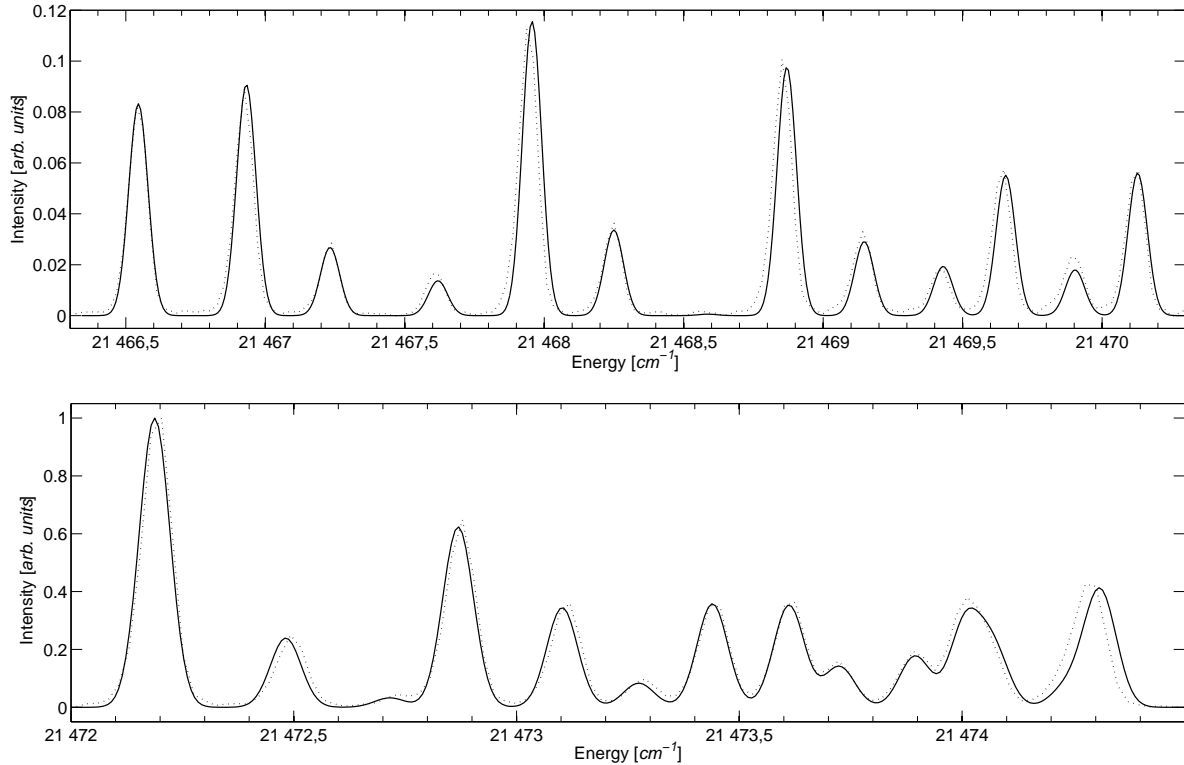
$$\begin{pmatrix} 1 & a'/a & b'/b & - \\ a'/a & 1 & a'b'/ab & b'/b \\ b'/b & a'b'/ab & 1 & a'/a \\ - & b'/b & a'/a & 1 \end{pmatrix} \quad (33)$$

and the final (J-state) hyperfine interaction matrix turns out as

$$\begin{pmatrix} 0.72546 & -0.73211 & 0.44613 & 0.00000 \\ 0.83014 & -0.18473 & 0.58167 & -0.43549 \\ -0.50586 & 0.58167 & 0.37356 & -0.71440 \\ 0.00000 & 0.51528 & 0.84529 & -0.52841 \end{pmatrix} \quad (34)$$

We also performed the corresponding re-scaling of the hyperfine interaction for the even levels. Finally, since the transition matrix elements were changed by less than one

Figure 2. Our synthetic *adjusted* spectrum (solid line) compared to experimental spectrum by Karlsson and Litzén [12] (dotted line). Upper spectrum is the hyperfine components of the $5s5d\ ^3D_2 - 5s4f\ ^3F_2^o$ transitions and the lower spectrum is the $^3D_2 - ^3F_3^o$.

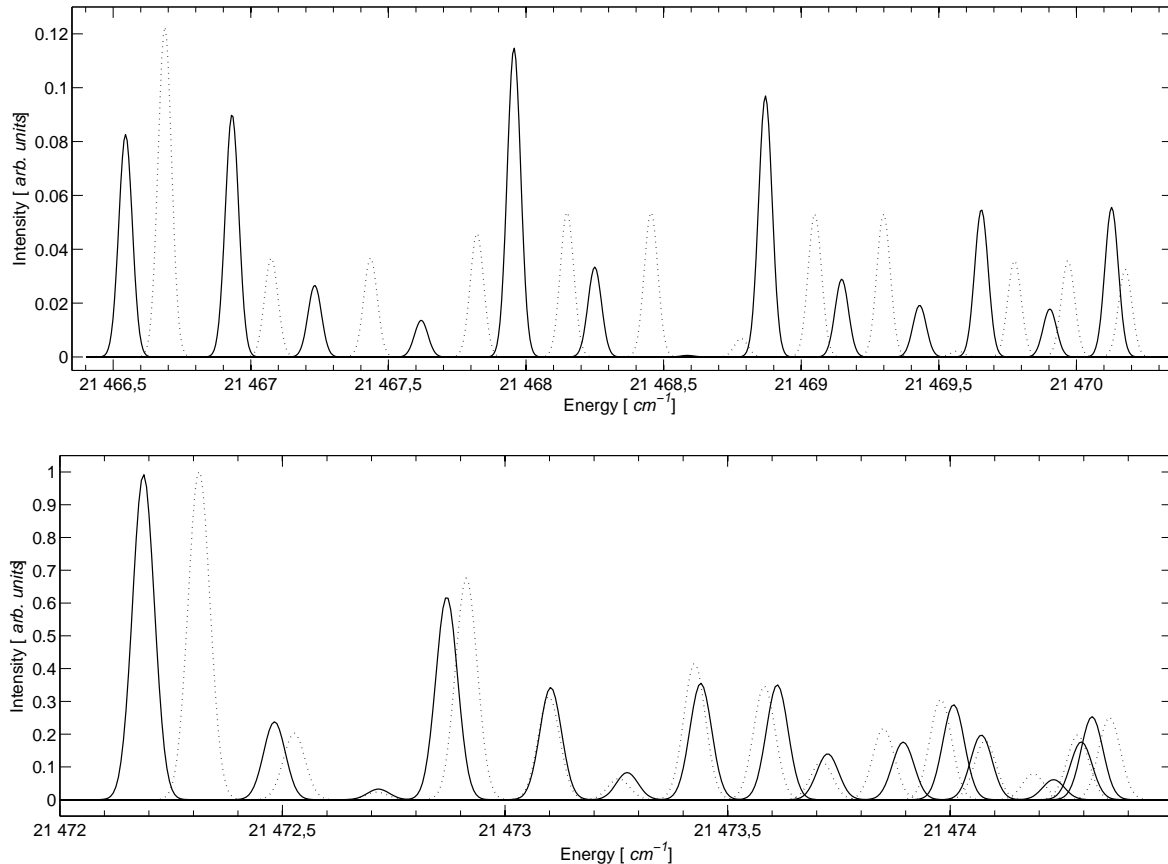


percent by this adjustment techniques, a value well within our uncertainty estimates, we did not include them.

In Figure 2 we present the *adjusted* spectrum (solid line) in comparison with the experimental by Karlsson and Litzén [12] (dotted line). Close agreement is found for both parts and there is only some very small differences in energies and intensities.

To investigate the influence of the off-diagonal hyperfine interaction, we also performed a calculation omitting this interaction. We call this the *adjusted diagonal* calculation and it is based on the same assumptions as made by Karlsson and Litzén [12] when they tried to understand the structure using A and B hyperfine constants. In Figure 3 we compared the synthetic spectrum from the *diagonal* calculation (dotted) to the *adjusted* one (solid). It is found that there are large differences between the two spectra for the $5s5d\ ^3D_2 - 5s4f\ ^3F_2^o$ transitions, not only in the position but foremost in the intensities. The differences are much smaller for the $5s5d\ ^3D_2 - 5s4f\ ^3F_3^o$ transitions but it is clear that the structure could not be described using diagonal hyperfine constants.

Figure 3. Comparison between a *diagonal* (dotted) and *adjusted* (solid) calculation. All the individual lines are plotted separately. The upper spectrum is the $5s5d\ ^3D_2 - 5s4f\ ^3F_2^o$ transitions and the lower is the $^3D_2 - ^3F_3^o$

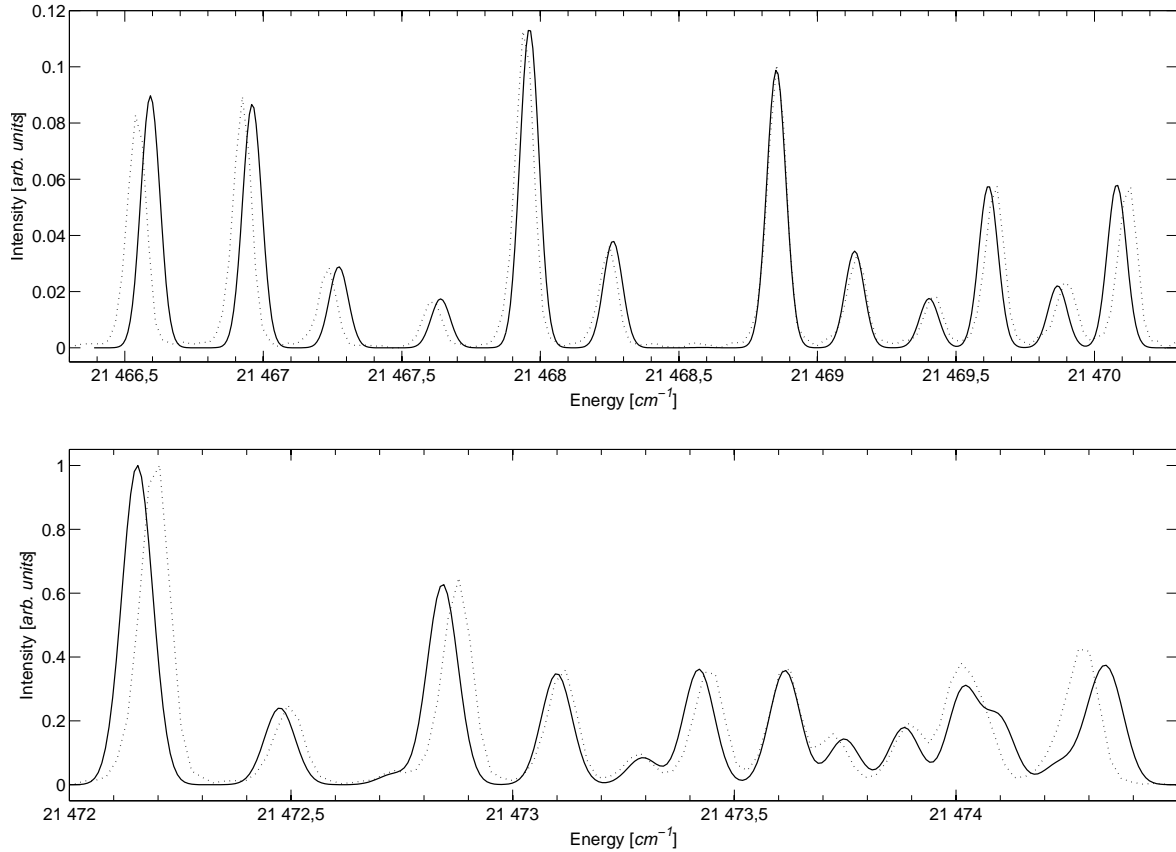


5.3. Large calculation

To try to achieve better *ab initio* results a second calculation was performed using a multi-reference set for the $5s4f$ optimization. We will refer to this calculation as the *large* whereas we will refer to the one discussed above as the *small* or *small adjusted*. The calculation followed the same steps as described in the section Method of Calculations except that the configuration space was created from the multi-reference configuration set $5s4f$, $5s5p$, $5p5d$ and $5d4f$. Using this model the number of configurations grow rapidly, and while running the calculation with the *AS4* set of orbitals some files generated by GRASP2K became larger than 2^{31} bytes, and therefore too large to handle for a 32 bit program. Therefore we had to stop at the *AS3* step and could not obtain certain convergence in this calculation. However, it was found for the *small* calculation that convergence was obtained both for energies and gf-values between *AS3* and *AS4* and it is therefore likely that we would have found convergence for the *large* calculation if the *AS4* calculation could have been performed.

It was found that the fine structure splitting in the *large* calculation was closer to

Figure 4. Our synthetic spectrum generated from the *large* calculation (solid line) compared to experimental spectrum by Karlsson and Litzén [12] (dotted line). Upper spectrum is the $5s5d\ ^3D_2 - 5s4f\ ^3F_2^o$ transitions and the lower spectrum is the $^3D_2 - ^3F_3^o$.

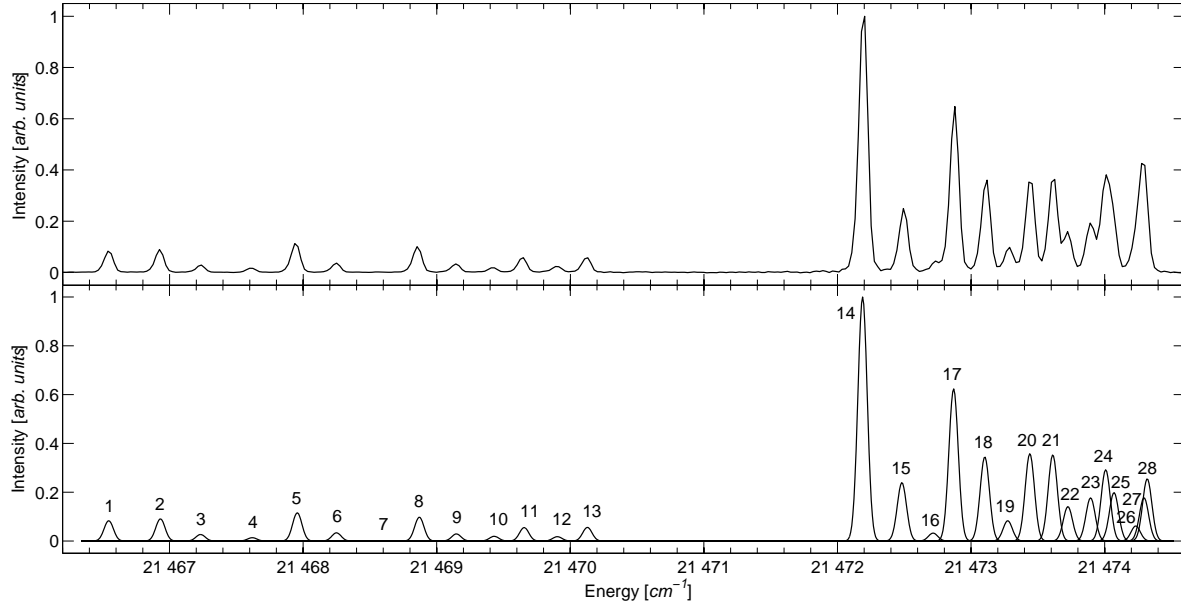


the experimental values than the *small*. The energy splitting between $5s4f\ ^3F_3^o$ and $^1F_3^o$ was calculated to 42.00cm^{-1} , further away from the experimental value of 51.14cm^{-1} than the prediction from the *small* calculation of 49.60cm^{-1} . Investigating the gf-values it was found that the two gauges were differing by 16% and that the $gf(^3D_2, ^3F_2^o)$ was almost identical to the value from the *small* calculations and the $gf(^3D_2, ^3F_3^o)$ was 4% smaller.

In Figure 4 we present our synthetic spectra from the *large* calculation (solid line) compared to the experimental spectra by Karlsson and Litzén [12] (dotted line). We have displayed the low energy, $5s5d\ ^3D_2 - 5s4f\ ^3F_2^o$, transition in the top panel, while the high energy, $5s5d\ ^3D_2 - 5s4f\ ^3F_3^o$, is displayed in the bottom one. It is clear that both part shows good agreement, in general, between experimental and our synthetic spectra.

In the low energy part of the spectrum we observe that the *large* and *small* calculation produces almost identical spectra. In the high end part we find a significant improvement from the *small* calculation and are in agreement with the *small adjusted*

Figure 5. Identification of lines. The upper spectrum is the synthetic spectrum from the *small adjusted*. In the lower spectrum are the 28 hyperfine transitions given a gaussian profile, plotted separately and numbered for easy identification in Table 6.



spectrum. Studying the expansion coefficients of the $(5s4f_{5/2})_3^o$ and $(5s4f_{7/2})_3^o$ CSF:s in the JSF of $5s4f \ ^3F_3^o$ it is found that they are 0.8411 and 0.5144 respectively, very close to 0.8419 and 0.5128 obtained from the *small adjusted* calculation. It is somehow surprising that the *large* calculation reproduce these mixing coefficient bearing in mind that the predicted energy splitting between $5s4f \ ^3F_3^o$ and $^1F_3^o$ are further from experimental value than the *small* calculation. To get a better understanding of this phenomenon, further investigations has to be performed concerning the optimization of the JSF:s.

5.4. Line Identification

In Table 6 we present the calculated hyperfine transitions. The energies are derived with the *small adjusted* calculation, and the *gf*-values comes from the *large*, *small adjusted* and *small adjusted diagonal* calculations respectively. The lines are numbered for easy identification in Figure 5.

Comparing gf_{adjust} and gf_{diag} , it is notable how much larger impact the off-diagonal hyperfine interaction has on the *gf*-values of the $5s5d \ ^3D_2 - 5s4f \ ^3F_2^o$ transition than on the $5s5d \ ^3D_2 - 5s4f \ ^3F_3^o$. As discussed by Andersson [10], this could be understood from the fact that the *gf* value of the former transition between the J-states are much larger than the one for the latter. Introducing a hyperfine mixing between these states will then have a much larger impact on the transitions involving $5s4f \ ^3F_2^o$ than $^3F_3^o$. This effect can, in addition to comparing the two rightmost columns in Table 6, also be

Table 6. gf-values from the *large*, *small adjusted* and *small adjusted diagonal* calculations. The energies of the transitions are from the *small adjusted* calculation.

#	3D		${}^3F^o$		E[cm^{-1}]	gf_{large}	gf_{adjust}	gf_{diag}
	J	F	J	F				
1	2	13/2	2	13/2	21466.5448	$8.37 \cdot 10^{-1}$	$8.23 \cdot 10^{-1}$	1.22
2	2	11/2	2	13/2	21466.9318	$8.09 \cdot 10^{-1}$	$8.98 \cdot 10^{-1}$	$3.67 \cdot 10^{-1}$
3	2	13/2	2	11/2	21467.2322	$2.69 \cdot 10^{-1}$	$2.65 \cdot 10^{-1}$	$3.67 \cdot 10^{-1}$
4	2	11/2	2	11/2	21467.6192	$1.62 \cdot 10^{-1}$	$1.35 \cdot 10^{-1}$	$4.59 \cdot 10^{-1}$
5	2	9/2	2	11/2	21467.9563	1.06	1.14	$5.36 \cdot 10^{-1}$
6	2	11/2	2	9/2	21468.2497	$3.55 \cdot 10^{-1}$	$3.33 \cdot 10^{-1}$	$5.36 \cdot 10^{-1}$
7	2	9/2	2	9/2	21468.5868	$1.11 \cdot 10^{-3}$	$5.71 \cdot 10^{-3}$	$6.88 \cdot 10^{-2}$
8	2	7/2	2	9/2	21468.8697	$9.23 \cdot 10^{-1}$	$9.65 \cdot 10^{-1}$	$5.29 \cdot 10^{-1}$
9	2	9/2	2	7/2	21469.1472	$3.21 \cdot 10^{-1}$	$2.88 \cdot 10^{-1}$	$5.29 \cdot 10^{-1}$
10	2	7/2	2	7/2	21469.4301	$1.64 \cdot 10^{-1}$	$1.91 \cdot 10^{-1}$	$2.16 \cdot 10^{-2}$
11	2	5/2	2	7/2	21469.6546	$5.38 \cdot 10^{-1}$	$5.45 \cdot 10^{-1}$	$3.57 \cdot 10^{-1}$
12	2	7/2	2	5/2	21469.9032	$2.06 \cdot 10^{-1}$	$1.78 \cdot 10^{-1}$	$3.57 \cdot 10^{-1}$
13	2	5/2	2	5/2	21470.1278	$5.42 \cdot 10^{-1}$	$5.53 \cdot 10^{-1}$	$3.24 \cdot 10^{-1}$
14	2	13/2	3	15/2	21472.1878	9.33	9.88	10.0
15	2	13/2	3	13/2	21472.4821	2.25	2.37	2.02
16	2	13/2	3	11/2	21472.7156	$3.06 \cdot 10^{-1}$	$3.22 \cdot 10^{-1}$	$2.31 \cdot 10^{-1}$
17	2	11/2	3	13/2	21472.8690	5.86	6.17	6.73
18	2	11/2	3	11/2	21473.1025	3.25	3.41	3.13
19	2	11/2	3	9/2	21473.2744	$7.86 \cdot 10^{-1}$	$8.23 \cdot 10^{-1}$	$6.37 \cdot 10^{-1}$
20	2	9/2	3	11/2	21473.4396	3.38	3.54	4.14
21	2	9/2	3	9/2	21473.6115	3.34	3.49	3.45
22	2	9/2	3	7/2	21473.7247	1.33	1.39	1.17
23	2	7/2	3	9/2	21473.8944	1.67	1.75	2.17
24	2	7/2	3	7/2	21474.0076	2.77	2.89	3.05
25	2	7/2	3	5/2	21474.0700	1.88	1.96	1.79
26	2	5/2	3	7/2	21474.2322	$5.82 \cdot 10^{-1}$	$6.08 \cdot 10^{-1}$	$7.86 \cdot 10^{-1}$
27	2	5/2	3	5/2	21474.2945	1.68	1.75	1.97
28	2	5/2	3	3/2	21474.3186	2.41	2.52	2.50

seen in Figure 3 where the complete and diagonal calculations are compared.

Comparing gf_{large} and gf_{adjust} we find that they are in most cases in fair agreement. Starting with the transitions from $5s4f {}^3F_3^o$ it is found that gf_{large} are 4-6% smaller than gf_{adjust} . This is due to the fact that the calculated gf -value between the JSF:s in the *large* calculation was about 4% smaller than the gf -value from the *small* calculation. The differences are larger comparing the transitions from $5s4f {}^3F_2^o$. The two calculated gf -values between the JSF:s were almost identical in the *large* and *small* calculation

and could therefore not have any impact on the differences between the calculated hyperfine dependent gf -values. The differences for these transitions are dominated by the variations in the calculated hyperfine interaction matrix elements. From Table 6 it is found that the differences in the gf -values for the strong transitions are in most cases well within 10%, which we would argue is in good agreement considering the large differences between these and the predicted values from the *diagonal* calculation. For the weaker transitions, the differences increases and for the weakest transition it is a factor of 5. Comparing with gf_{diag} it is found that the off-diagonal hyperfine interaction introduces strong cancelation effects for this transition. This cancelation emerges from the mixing with the ${}^3F_3^o$ hyperfine level which has a gf_{diag} value to the same lower hyperfine level which is 50 times larger. This makes the gf -value very sensitive to even a very small difference in the off-diagonal hyperfine interaction matrix element, making an accurate prediction extremely difficult.

Comparing the synthetic spectra from the *large* and the *small adjusted* calculation, which both reproduces quite well the experimental spectrum (Figure 4 and 2), it is clear that the latter is in better agreement and the gf_{adjust} should therefore be considered as the most accurate.

Conclusions

We have investigated the hyperfine structure of the $5s5d\ {}^3D_2 - 5s4f\ {}^3F_{2,3}^o$ transitions in In II. The structure of the spectrum for these transitions is heavily dependent on off-diagonal hyperfine interaction. We have performed large scale calculations using the MCDHF method and our synthetic spectrum was found to be in close agreement with experiment. We also performed calculations using a much smaller configuration space and derived a semi-empirical method which could correct for the inaccurate term splitting in the $5s4f$ configuration using an experimentally determined hyperfine interaction constant for the $5s4f\ {}^1F_3^o$ level. This in turn allowed us to adjust both the diagonal and off-diagonal hyperfine interaction matrix elements. It was found that the synthetic spectrum obtained using this procedure was in excellent agreement with experiment.

An accurate method for determining the hyperfine structure of transitions where off-diagonal hyperfine interaction has a large impact could be an important aid in abundance determinations using stellar spectra, or the identification of lines in high resolution spectroscopy. For this purpose, the energy and the gf -value of all the $5s5d\ {}^3D_2 - 5s4f\ {}^3F_{2,3}^o$ transitions are given.

Acknowledgment

We would like to thank Ulf Litzén and Hans Sabel of the Atomic astrophysics group at the Astronomy department, Lund University for letting us use their experimental spectrum of In II. We would also like to thank one of the referees for helpful comments

and crucial corrections that helped us substantially improve this paper.

This work was supported by *China Postdoctoral Science Foundation*, the *Swedish Research Council* and *Kungliga Fysiografiska Sällskapet i Lund*. One of the authors, Jon Grumer, would also like to thank *Stiftelsen Aagot och Christian Storjohanns minnesfond för värmländsk kultur* and *Stiftelsen Carl Axel Bergstrand* for the economical support that made it possible to spend time at the Fudan University in Shanghai. The same author would also like to thank professor Yaming Zou, head of the Shanghai EBIT laboratory at Fudan university, for arranging so that he could visit her group and perform this work.

References

- [1] A. J. Booth and D. E. Blackwell *Mon. Note Royal. Astron. Soc.* **204** 777 (1983)
- [2] C. M. Jomaron, M. M. Dworetzky and C. S. Allen *Mon. Not. Royal Astron. Soc.* **303** 7 (1999)
- [3] H. Karlsson and U. Litzén *J. Phys. B: At. Mol. Opt. Phys.* **33** 2929 (2000)
- [4] R. J. Blackwell-Whitehead, J. C. Pickering, O. Pearse and G. Naves *Astrophys. J. Suppl.* **157** 402 (2005)
- [5] V. V. Smith and G. Wallerstein *Astrophys. J.* **533** L139 (1983)
- [6] V. V. Smith and D. L. Lambert *Publ. Astron. Soc. Pacific* **96** 226 (1984)
- [7] H. Nilsson and S. Ivarsson *Astron. & Astrophys.* **492** 609 (2008)
- [8] A. Aboussaïd, M. Carleer, D. Hurtmans, E. Biémont and M.R. Godefroid *Phys. Scr.* **53** 28 (1996)
- [9] M. Andersson, P. Jönsson and H. Sabel *J. Phys. B: At. Mol. Opt. Phys.* **39** 4239 (2006)
- [10] M. Andersson *Phys. Scr.* **T134** 014021 (2009)
- [11] P. Jönsson, X. Heb, C. Froese Fischer and I.P. Grant *Comp. Phys. Com.* **177** 597 (2007)
- [12] H. Karlsson and U. Litzén *J. Phys. B: At. Mol. Opt. Phys.* **34** 4475 (2001)
- [13] F. Paschen and J. S. Campbell *Annalen der Physik* **31** 29 (1938)
- [14] E. Peik, G. Holleman and H. Walther *Phys. Rev. A* **49** 402 (1993)
- [15] P. L. Larkins and P. Hannaford *Z. Phys. D* **27** 313 (1993)
- [16] P. Jönsson and M. Andersson *J. Phys. B: At. Mol. Opt. Phys.* **40** 2417 (2007)
- [17] J. von Zanthier, J. Abel, T. Becker, M. Fries, E. Peik, H. Walther, R. Hozwarth, J. Reichert, T. Udem, T.W. Hänsch, A. Y. Nevsky, M. N. Skvortsov and S. N. Bagayev *Optics Communication* **166** 57 (1999)
- [18] J. von Zanthier, T. Becker, M. Eichenseer, A. Y. Nevsky, C. Schwedes, E. Peik, H. Walther, R. Hozwarth, J. Reichert, T. Udem, T.W. Hänsch, P. V. Pokasov, M. N. Skvortsov and S. N. Bagayev *Optics Letter* **25** 1729 (2000)
- [19] J.P. Marques, F. Parente, P. Indelicato *Phys Rev A* **47** 929 (1993)
- [20] T. Brage, P.G. Judge, A. Aboussaïd, M.R. Godefroid, P. Jönsson, A. Ynnerman, C.F. Fischer and D.S. Leckrone *Astrophys. J* **500** 507 (1998)
- [21] S. Schippers, E.W. Schimdt, D. Bernhardt, D. Yu, A. Müller, M. Lestinsky, D.A. Orlov, M. Greiser, R. Repnow and A. Wolf *Phys. Rev. Lett.* **98** 033001 (2007)
- [22] K.T. Cheng, M.H. Chen and W.R. Johnson *Phys Rev A* **77** 052504 (2008)
- [23] M. Andersson, Y. Zou, R. Hutton and T. Brage *Phys. Rev. A* **79** 032501 (2009)
- [24] J.P. Marques, F. Parente, P. Indelicato *At. Data Nucl. Data Tables* **55** 157 (1993)
- [25] T. Rosenband, P.O. Schmidt, D.B. Hume, W.M. Itano, T.M. Fortier, J.E. Stalnaker, K. Kim, S.A. Diddams, J.C.J. Koelemeij, J.C. Berquist and D.J. Wineland *Phys. Rev. Lett.* **98** 220801 (2007)
- [26] M. Andersson, Y. Zou, R. Hutton and T. Brage *J. Phys. B* (Submitted)
- [27] Y. Liu, R. Hutton, Y. Zou, M. Andersson and T. Brage *J. Phys. B* **39** 3147 (2006)
- [28] W.R. Johnson, K.T. Cheng and D.R. Plante *Phys. Rev. A* **55** 2728 (1997)
- [29] P. Indelicato, F. Parente and R. Marrus *Phys. Rev. A* **40** 3505 (1989)

- [30] L. Engström, C. Jupén, B. Denne, S. Huldt, T.M. Weng, P. Kaijser, U. Litzén, and I. Martinson *J. Phys. B* **13** L143 (1980)
- [31] B. Denne, S. Huldt, J. Pihl and R. Hallin *Phys. Scr.* **22** 45 (1980)
- [32] A.E. Livingston and S.J. Hinterlong *Nucl. Instrum. Methods* **202** 103 (1982)
- [33] R.W. Dunford, C.J. Liu, J. Last, N. Berrah-Mansour, R. Vondrasek, D.A. Church, and L.J. Curtis *Phys. Rev. A* **44** 764 (1991)
- [34] H. Bergström, C. Levinson, H. Lundberg, S. Svanberg, C.G. Wahlström and Z.Y. Yuan *Phys Rev A* **33** 2387 (1986)
- [35] K. Yao, M. Andersson, T. Brage, R. Hutton, P. Jönsson and Y. Zou *Phys. Rev. Lett.* **97** 183001 (2006)
- [36] K. Yao, M. Andersson, T. Brage, R. Hutton, P. Jönsson and Y. Zou *Phys. Rev. Lett.* **98** 269903 (2007)
- [37] E. Träbert, P. Beiersdorfer and G.V. Brown *Phys. Rev. Lett.* **98** 263001 (2007)
- [38] R. Marrus, A. Simionovici, P. Indelicato, D.D. Dietrich, P. Charles, J-P Briand, K. Finlayson, F. Bosch, D. Liesen and F. Parente *Phys. Rev. Lett.* **63** 502 (1989)
- [39] I. Lindgren and A. Rosén *Case Stud. At. Phys.* **4** 97 (1974)
- [40] R.L. Kurucz *Phys. Scr.* **T47** 110 (1993)
- [41] R.D. Cowan *The Theory of Atomic Structure and Spectra* (University of California Press, 1981)
- [42] I. P. Grant "Relativistic Quantum Theory of Atoms and Molecules: Theory and Computation (Springer Series on Atomic, Optical and Plasma Physics, Berlin: Springer 2007)
- [43] B. J. McKenzie, I. P. Grant and P. H. Norrington *Comput. Phys. Commun.* **21** 233 (1980)
- [44] J. Olsen, M Godefroid, P. Jönsson and P. Å. Malmqvist and C Froese Fischer", *Phys. Rev. E* **52** 4499 (1995)
- [45] I. P. Grant *J. Phys. B: At. Mol. Phys.* **7** 1458 (1974)
- [46] B. O. Roos, P. R. Taylor and P. E. M. Siegbahn *Chem. Phys.* **48** 157 (1980)
- [47] J. Olsen, B. O. Roos, P. Jørgensen and H. J. Aa. Jensen *J. Chem. Phys.* **89** 2185 (1988)
- [48] T. Brage and C. Froese Fischer *Phys. Scr.* **T47** 18 (1993)
- [49] M. Andersson and P. Jönsson *Comp. Phys. Com.* **178** 156 (2008)
- [50] I. Lindgren and J. Morrison *Atomic Many-Body Theor*, Vol 13, *Springer Series in Chemical Physics* (Springer-Verlag, Berlin 1982)
- [51] P. Jönsson *Phys. Scr.* **48** 678 (1993)
- [52] C.F. Fischer, G. Tachiev, G. Gaigalas and M.R. Godefroid *Comput. Phys. Commun.* **176** 559 (2007)